

PROMSAR: A backward Monte Carlo spherical RTM for the analysis of DOAS remote sensing measurements

E. Palazzi^{a,*}, A. Petritoli^a, G. Giovanelli^a, I. Kostadinov^{a,b}, D. Bortoli^{a,c},
F. Ravegnani^a, S.S. Sackey^d

^a *Institute of Atmospheric Sciences and Climate (ISAC) of the Italian National Research Council (CNR), 101, Gobetti Road, 40129 Bologna, Italy*

^b *STIL-Bulgaria Academy Science Department, Stara Zagora, Bulgaria*

^c *CGE-UE, University of Evora, Portugal*

^d *Laser and Fiber Optics Centre, University of Cape Coast, Ghana*

Received 28 October 2004; received in revised form 5 May 2005; accepted 5 May 2005

Abstract

A correct interpretation of diffuse solar radiation measurements made by Differential Optical Absorption Spectroscopy (DOAS) remote sensors require the use of radiative transfer models of the atmosphere.

The simplest models consider radiation scattering in the atmosphere as a single scattering process. More realistic atmospheric models are those which consider multiple scattering and their application is useful and essential for the analysis of zenith and off-axis measurements regarding the lowest layers of the atmosphere, such as the boundary layer. These are characterized by the highest values of air density and quantities of particles and aerosols acting as scattering nuclei.

A new atmospheric model, PROcessing of Multi-Scattered Atmospheric Radiation (PROMSAR), which includes multiple Rayleigh and Mie scattering, has recently been developed at ISAC-CNR. It is based on a backward Monte Carlo technique which is very suitable for studying the various interactions taking place in a complex and non-homogeneous system like the terrestrial atmosphere. PROMSAR code calculates the mean path of the radiation within each layer in which the atmosphere is sub-divided taking into account the large variety of processes that solar radiation undergoes during propagation through the atmosphere. This quantity is then employed to work out the Air Mass Factor (AMF) of several trace gases, to simulate in zenith and off-axis configurations their slant column amounts and to calculate the weighting functions from which informations about the gas vertical distribution is obtained using inversion methods.

Results from the model, simulations and comparisons with actual slant column measurements are presented and discussed.

© 2005 COSPAR. Published by Elsevier Ltd. All rights reserved.

Keywords: Remote sensing; Radiative transfer models; Air mass factor; Multiple scattering; Monte Carlo simulation

1. Introduction

DOAS methodology using the sun as source of radiation has proven to be one of the major tools for the

determination of the slant columns of several atmospheric trace gases (Noxon, 1975; Platt et al., 1997; Platt, 1999; Solomon et al., 1987). A DOAS spectrometer directed along the line of sight (LOS) in zenith or off-axis directions observes the optical density of trace gas absorption bands via the scattering of sunlight at different layers of the atmosphere. DOAS methodology is based on the application of the Bouguer–Beer–Lambert law which can be written as follows as applied to the atmosphere:

* Corresponding author. Tel.: +390516399584; fax: +390516399652.

E-mail addresses: e.palazzi@isac.cnr.it (E. Palazzi), a.petriloti@isac.cnr.it (A. Petritoli), g.giovanelli@isac.cnr.it (G. Giovanelli), i.kostadinov@isac.cnr.it (I. Kostadinov), d.bortoli@isac.cnr.it (D. Bortoli), f.ravegnani@isac.cnr.it (F. Ravegnani), s.sackey@isac.cnr.it (S.S. Sackey).

$$I_\lambda = I_\lambda(0) \cdot \exp \left[- \int_{S_\rho(\text{SZA}, \lambda)} \sigma_{\lambda g} \cdot \rho_g(s) \cdot ds \right] \\ = I_\lambda(0) \cdot \exp(-D), \quad (1)$$

where $I_\lambda(0)$ denotes the initial intensity emitted by the source of radiation, I_λ is the intensity of the radiation after it passes through a layer of thickness s , while the species to be measured is present at the concentration ρ_g . The quantity $\sigma_{\lambda g}$ denotes the gas absorption cross section at wavelength λ , $S_\rho(\text{SZA}, \lambda)$ is the atmospheric radiation path and D is the optical density of a layer of a given species.

From the optical density D estimated from measurements, the gas slant column $\text{SC}_g(\text{SZA}, \lambda)$ can be computed by applying the DOAS methodology as shown in Eqs. (2) and (3)

$$\ln \left[\frac{I_\lambda(0)}{I_\lambda} \right] = \sigma_{\lambda g} \cdot \int_{S_\rho(\text{SZA}, \lambda)} \rho_g(s) \cdot ds, \quad (2)$$

$$\text{SC}_g(\text{SZA}, \lambda) = \int_{S_\rho(\text{SZA}, \lambda)} \rho_g(s) \cdot ds. \quad (3)$$

The quantities $\sigma_{\lambda g}$, $I_\lambda(0)$, I_λ , ρ_g , s , $S_\rho(\text{SZA}, \lambda)$ in the Eqs. (2) and (3) have the same meaning as defined in Eq. (1). The slant column is a function of the solar zenith angle (SZA), the wavelength of radiation (λ) and the detector line of sight (LOS). It also depends on the vertical structure of the atmosphere. A new quantity must be introduced to compare measurements under different viewing geometries, which is the vertically integrated trace gas concentration (vertical column). Modelling the physical process of radiation transport through radiative transfer models of the atmosphere allows determination of the AMF of atmospheric trace gases, which is used to relate the slant column of a trace gas to its vertical column. The AMF can be written as follows:

$$\text{AMF}_g(\text{SZA}, \lambda) = \frac{\text{SC}_g(\text{SZA}, \lambda)}{\text{VC}_g}, \quad (4)$$

where VC_g is the vertical column amount of the species. The AMF is a function of solar zenith angle and wavelength and depends to some extent on the assumptions of the relative vertical trace gas profiles and air density (Marquard and Platt, 1997; Solomon et al., 1987). By using AMF computed by models, not only could the vertical column of a trace gas be retrieved but also the weighting functions, W_{z_i} , from which information about the gas vertical distribution is obtained using inversion methods:

$$W_{z_i} = \frac{\partial \text{SC}_g(\text{SZA}, \lambda)}{\partial \rho_{g_{z_i}}}. \quad (5)$$

PROMSAR is a new radiative transfer model (Palazzi, 2003) based on a backward Monte Carlo technique that considers multiple scattering for the evaluation of scattered radiation measurements. This ensures a more

realistic description of the radiation transport in the atmosphere than that given by single scattering models (Giovannelli et al., 1989, 1990, 1992). Consequently, it allows for a more accurate interpretation of zenith sky and off-axis measurements from DOAS spectrometers measuring diffuse UV–visible solar radiation.

In this actual form the PROMSAR RTM does not take into account the refraction. The main quantity computed by PROMSAR is the mean path of photons through the atmosphere layer by layer. This is very important because the ability to correctly compute AMFs depends on how well the optical path of light collected by the receiver is understood and computed by models. Once the photon path inside each layer has been computed, it is used to work out the AMF of a trace gas whose vertical profile is requested. It is then used to simulate its slant column amount and compute the weighting functions from which information about the vertical profile of the absorber in atmosphere is obtained using inversion methods (McKenzie et al., 1991; Preston et al., 1998; Petritoli, 1998; Petritoli et al., 2002, 2004). The trace gas slant column computed by PROMSAR is given by the equation:

$$\text{SC}(\text{SZA}, \lambda) = \sum_{l=1}^L \Delta S_{\text{mult}}(l, \text{SZA}, \lambda) \cdot \rho_g(l), \quad (6)$$

where ρ_g is the gas concentration in units of molec/cm³ which is assumed to be constant in each layer and ΔS_{mult} is the mean photon path into the l th layer computed by PROMSAR in units of cm (the subscript “mult” indicates “multiple scattering”). This changes according to SZA, λ , and the vertical structure of the atmosphere. L indicates the layer at the top of atmosphere.

The air mass factor can be computed by the model and is defined as:

$$\text{AMF}(\text{SZA}, \lambda) = \frac{\sum_{l=1}^L \Delta S_{\text{mult}}(l, \text{SZA}, \lambda) \cdot \rho_g(l)}{\Delta z \cdot \sum_{l=1}^L \rho_g(l)}, \quad (7)$$

where ρ_g and ΔS_{mult} have the same meaning as defined in Eq. (6) and Δz represents the altitude step.

2. The PROMSAR code for the Monte Carlo simulation of radiation transport in the atmosphere

2.1. Model description

PROMSAR is a backward Monte Carlo code for atmospheric radiative transfer. It is suitable for the ultraviolet–visible region of the electromagnetic spectrum in which the radiation source is considered to be a parallel flux incident on the upper boundary with a given direction. In what follows we refer to the solar radiation as the source impinging on the top boundary and to the atmosphere as the medium even though the

algorithm can have more general applications. The atmosphere is modelled with a spherical 2D multi-layer user defined geometry in which the optical parameters (e.g., the extinction coefficients and the phase functions) can vary from layer to layer.

The model has been partially validated by comparison with other radiative transfer models (Palazzi, 2003; Palazzi et al., 2004). Data available in the report of Hendrick et al., 2003, have also been used to perform this validation.

Since Monte Carlo methods rest on the fact that radiation is made up of small packets of energy referred to as photons, the propagation of solar radiation can be treated on the same basis as the transport of particles, that is, by the use of probabilistic methods. Monte Carlo methods are generally known for being easier to implement compared to other computational methods for atmospheric radiative transfer such as the discrete ordinate method implemented in the DISORT model (Stamnes et al., 1988) or the method of finite differences used in the GOMETRAN RTM (Rosanov et al., 1998). The Monte Carlo approach consists of using probabilistic concepts and methods to simulate the trajectories of individual photons in the atmosphere. A statistical weight is assigned to each photon and reduced at each interaction. A photon history is terminated when the statistical weight falls below a specified threshold value (W_{Tr}).

This method is met on the linking up of a series of probability functions (Roberti, 1997, and references therein) from which the variables of interest for the simulation are randomly sampled (see Sections 2.1.1, 2.1.2). The Monte Carlo method is well adapted to situations involving atmospheres whose properties change with altitude and for phase functions that are highly anisotropic.

In the backward Monte Carlo scheme implemented in PROMSAR the procedure for each photon is initiated by releasing the photon from the spectrometer. This is the point where it is to be collected and with a direction opposite to that in which the photon would physically propagate and coinciding with the spectrometer LOS. In the backward Monte Carlo scheme, the first collision is the last in the temporal physical sequence. As demonstrated by Collins et al. (1972), utilization of a backward Monte Carlo approach eliminates certain problems involved in a forward Monte Carlo approach.

The real disadvantages of every Monte Carlo method are a lower accuracy and a longer computational time. Together with the photon weight threshold, the determining parameter to obtain statistically significant results is the number of photon used in the simulation, N (Roberti, 1997). However in a number of situations if biasing schemes are not used, the computational time can increase disproportionately despite an optimal choice for N and W_{Tr} . As a result most of the existing

Monte Carlo methods rely on variance reducing schemes to reduce computational time and keep the statistical oscillations relatively small (Roberti, 1997). The reducing variance scheme implemented in PROMSAR code is known as forced collision technique. This means that a collision is forced before the photon escapes the atmosphere.

2.1.1. Optical distance between collisions

Two methods are used to sample the distances between the receiver and the n th collision point as well as the successive collisions that occur along the photon's backward path (free optical path). If the photon extended path intersects the surface, the free optical path is sampled from the distribution:

$$\tau = -\ln(1 - r), \quad (8)$$

where r is a random number sampled from a uniform distribution between $[0, 1]$. If τ is greater than the optical distance along the path from the actual position of the photon to the ground surface, a reflection is forced. The statistical weight is then multiplied by the albedo for the ground surface. If τ is less than the optical distance to the ground surface, a collision is considered to occur at the altitude where the sampled free optical path equals the optical distance. The photon is forced to scatter at this point and the photon weight is multiplied by the ratio between the scattering coefficient and the sum of the scattering and absorption coefficients (see Section 2.1.1) evaluated for the collision altitude.

If the photon extended path do not intersect the ground surface, a collision is forced before the photon escapes the atmosphere by selecting τ from the truncated exponential distribution (Collins et al., 1972), so that,

$$\tau = -\ln\{1 - r[1 - \exp(-\tau_{max})]\}, \quad (9)$$

where r is a random number sampled from a uniform distribution between $[0, 1]$ and τ_{max} is the optical distance along the path to the upper bound of atmosphere. This can be computed through the knowledge of the aerosol and molecules scattering coefficient for each layer supplied by the MODRAN code libraries. In this case, the biasing forced collision technique has been used in the sampling of the free optical path in order to reduce the computational time and keeping the statistical oscillations relatively small. When the collision is forced to occur before the photon escapes the atmosphere, the photon statistical weight before collision, w_{n-1} , is adjusted to remove the bias introduced by forcing the collision, as in the following expression:

$$w_n = w_{n-1} \cdot [1 - \exp(-\tau_{max})]. \quad (10)$$

It should be noted that the factor $[1 - \exp(-\tau_{max})]$ is always less than unity and should produce a smaller variance than that produced when using unforced sampling as in Eq. (8).

After the distance covered before collision is calculated, one of the three following scenarios can occur.

1. The photon will cross a layer before interaction with the medium so that it enters another layer with unchanged direction. A new free optical path will be calculated taking into account the distance already travelled.
2. If a collision occurs then a scattering event will be forced to happen. The corresponding bias is removed by the multiplication of the photon weight with the factor $(1 - W_{\text{ABS}})$. This represents the probability of photon survival and W_{ABS} is the fraction of the photon weight corresponding to its absorption by molecules in the current position of the photon.
3. If the trajectory of the photon meets the surface then a reflection will be forced to happen. The photon statistical weight is then multiplied by the surface albedo at the point of reflection.

The procedure above is repeated until the photon weight becomes smaller than the threshold value and the photon is eliminated.

2.1.2. Selection of scattering event

For each collision, the type of scattering, be it Rayleigh or Mie, is determined at random from a knowledge of the ratio of the Rayleigh (Mie) scattering coefficient to the sum of the Rayleigh and Mie scattering coefficients (total scattering coefficient) at the collision altitude. If

$$r \leq \frac{\text{XMS}}{\text{XAS} + \text{XMS}}, \quad (11)$$

the scattered component is a molecule and Rayleigh scattering has occurred, otherwise Mie scattering has occurred as the scattered component is an aerosol. In Eq. (11), r is a random number sampled from a uniform distribution between $[0, 1]$, XMS is the scattering coefficient for molecules (Rayleigh scattering coefficient) and XAS is the aerosol scattering coefficient (Mie scattering coefficient).

Due to the fact that the scattering of an individual photon is a stochastic process with the Rayleigh or Mie phase function being the probability function for scattering at a given angle, the scattering angle, θ_{scat} , can be obtained by randomly sampling its cosine, $\cos(\theta_{\text{scat}})$ from the appropriate phase function (Rayleigh or Mie phase functions), being careful to reduce as much as possible the time needed for extracting such a value.

2.2. The atmospheric scenarios

An input data library is assumed to be read by PROMSAR to build-up the appropriate probability distributions. For this purpose the radiance-transmittance MODTRAN code (Berk et al., 1999) has been conve-

niently adapted as a source of the input data library so as to exploit the rich of informations of the code as it has a large variety of atmospheric situations.

A wide range of atmospheric scenarios and therefore climatologic choices are available in MODTRAN. It makes provision for six reference atmospheres (tropical model, mid-latitude summer model, mid-latitude winter model, sub-arctic summer model, sub-arctic winter model, Standard US 1976 model) with each defined by temperature, pressure, molecular density and mixing ratios of major radiating atmospheric gases all as a function of altitude. The altitude increments are 1 km between 0 and 25 km, 2.5 km between 25 and 50 km and 5 km between 50 and 120 km. MODTRAN also allows the user to define an atmospheric profile with any specified set of parameters. The values corresponding to the physical quantities of interest are assigned to the lower and the upper height of every layer located between two altitude increments. Representatives of atmospheric aerosol, cloud and rain models are provided within the MODTRAN code with options to replace them with user-modelled or measured values. With regard to aerosol, the variation of their optical properties with altitude is modelled by dividing the atmosphere into four regions of height each having a different type of aerosol. These regions are the boundary or mixing layer (0–2 km), the upper troposphere (2–10 km), the lower stratosphere (10–30 km), and the upper atmosphere (30–100 km). A different atmospheric model with differing wavelength dependencies is used for each of the four altitude regions. The MODTRAN package includes several parameters to define aerosol profiles in the atmosphere. The most important of these parameters are the type of aerosol and the visibility. There are several types of aerosol available based on common aerosol mixtures that are found in most terrestrial conditions. These generate the following aerosol models: rural, urban, maritime, tropospheric, fog, wind dependent desert. The second important aerosol parameter, visibility, is used to define the amount of the aerosol in the atmosphere.

The data supplied by MODTRAN code have been adapted to built up a series of input data libraries for different aerosols, seasonal and latitude models to be read and processed by PROMSAR. Each of these input libraries contain the number of atmospheric layers and the values of the altitude increments for every atmospheric layer. It also contains the Mie phase functions, the aerosol scattering and absorption coefficients, the absorption and scattering coefficients of the gas compounds and the refraction indexes.

Moreover, certain parameters that are not included in the input library describing the atmospheric scenario can be set out by the user at the beginning of the simulation. These include the number of photons to be processed, the altitude where the instrument is placed (as it is possible to simulate a ground-based spectrometer or a spectrometer

installed on board an aircraft) and its line of sight, the photon weight threshold, the range of solar zenith angles and the surface albedo value. The user can also define the atmospheric layering, the upper limit of atmosphere, the number of layers and the altitude increments regardless of the MODTRAN code atmospheric grid.

3. Results and discussion

3.1. Zenith and off-axis viewing geometries

In this section, some simulations of PROMSAR code in an urban aerosol model are presented and discussed.

Due to the flexibility of MODTRAN, for a given atmospheric model PROMSAR works out the mean path of radiation layer by layer within the user defined grid and uses it to calculate the air mass factor and the slant column of an atmospheric gas. The trace gas vertical profile must be known a priori in order to compute the AMF and SC.

In this paper the gas of interest is nitrogen dioxide, NO₂, whose vertical profile, as displayed in Fig. 1, has been obtained by adding to the gas mid-latitude climatological concentration values a mean concentration of 10 ppb (corresponding to a value of about 2.65E + 11 molec/cm³) in the first two kilometres (boundary layer). Two simulations have been executed which differ from each other only by the different viewing geometry set for the ground-based spectrometer. The first is the zenith-sky looking configuration (LOS = 0°) and the second is the off-axis configuration in which the spectrometer collects light in a direction that is not vertical. In this case a line of sight of 85° (LOS = 85°) has been set. The simulations have been performed using the MODTRAN urban extinction model with a visibility value of 5 km and a wavelength of 440 nm. The surface albedo value has been set at 0.3 and the relative azimuth angle is 0°. The values of the air mass factors and slant columns of NO₂ calculated by PROMSAR can be obtained in Fig. 2. It can be observed in Fig. 2

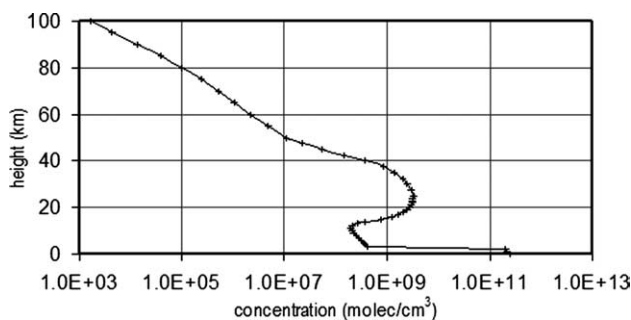


Fig. 1. NO₂ atmospheric vertical profile. The stratospheric bulk at 25 km corresponds to a concentration of 3.34E + 09 molec/cm³. A mean concentration of 10 ppb has been added in the first 2 km corresponding to a value of about 2.65E + 11 molec/cm³.

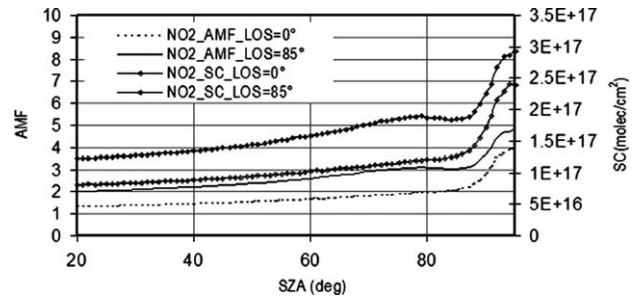


Fig. 2. NO₂ air mass factors (AMFs) in the left axis and slant columns (SCs) in the right axis. This is simulated by PROMSAR for a zenith-sky (LOS = 0°) and off-axis (LOS = 85°) looking spectrometer placed at ground level and plotted as a function of solar zenith angle (from 20° to 95°). The atmospheric model is the urban extinction model with visibility = 5 km and $\lambda = 440$ nm.

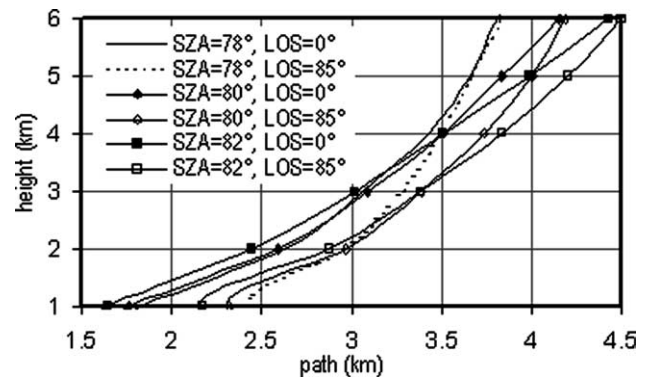


Fig. 3. Paths of solar radiation into 1-km-thick atmospheric layers (from the ground till 6 km) for SZA = 78°, 80°, 82° and for two different spectrometer's viewing geometries: LOS = 0° and LOS = 85°.

that the values of AMF and SC computed when LOS = 85° are higher than that computed when LOS = 0°. This is due to the fact that the path of radiation through the atmosphere and especially through the first atmospheric layers is longer for an off-axis observation. The photon path computed by PROMSAR layer by layer within the first five kilometres is displayed in Fig. 3 for three solar zenith angles around 80° and for the two lines of sight used in the simulation. As mentioned, Fig. 3 indicates that for the same SZA the photon path computed by PROMSAR for LOS = 85° are higher than that computed for LOS = 0°, in agreement with observations made in Fig. 2. A sloping collecting direction makes an atmospheric layer geometrically and optically thicker than a zenith sky direction. This means that the probability of interaction between the solar radiation and the atmospheric components increases as well as the path crossed by the radiation in that layer.

3.2. The dependence of the computed photon path on the atmospheric model

Some calculations of the photon paths computed by PROMSAR within each atmospheric layer are presented

in order to point out their dependence on the atmospheric models used in the simulation. The different models are distinguished from each other and for the kind of extinction and the visibility value used, both determined by the aerosol properties (see Section 2.2). The paths of each photon in every km-thick layer for $SZA = 30^\circ$ are displayed in Fig. 4 for two different atmospheric models: the rural and urban models.

The rural model is intended to represent the aerosol conditions one finds in the continental areas where the atmosphere is not directly influenced by urban and/or industrial aerosols sources. For this scenario the aerosols are assumed to be composed of 70% water-soluble substance (ammonium, calcium sulphate and organic compounds) and 30% dust-like aerosols. For an urban area the rural aerosol background is modified by the addition of aerosols from combustion products and industrial sources. The urban aerosol model was therefore taken to be a mixture of the rural aerosol and carbonaceous aerosols.

It can be observed in Fig. 4 that the photon paths computed for the rural model are higher than those for the urban model except for higher altitudes where the curves blend gradually to the same value. The reason for the difference at low altitudes is that the urban aerosol absorbs much more than the rural leading to a reduced path length in the urban model. Fig. 5 shows the aerosol absorption coefficients (XAA) as a function of the altitude.

It can also be seen in Fig. 4 that the value of the atmospheric paths increases with the altitude over about the first few kilometres until reaching a maximum. It then decreases and stabilizes to a constant value. This trend strongly depends on the fact that a zenith-sky looking geometry has been set so that the photons are released by the spectrometer (backward Monte Carlo scheme) along the vertical. In any case this is not an artificial effect due to the backward approach as it is what is expected of light in order to be detected by the instru-

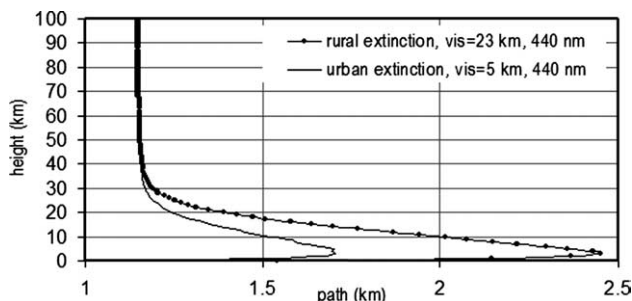


Fig. 4. Paths of solar radiation into 1-km-thick atmospheric layers for $SZA = 30^\circ$ with the ground-based spectrometer in zenith sky geometry. Two different input atmospheric models have been read and processed by PROMSAR: the “rural extinction model, visibility = 23 km, $\lambda = 440$ nm” and the “urban extinction model, visibility = 5 km, $\lambda = 440$ nm”.

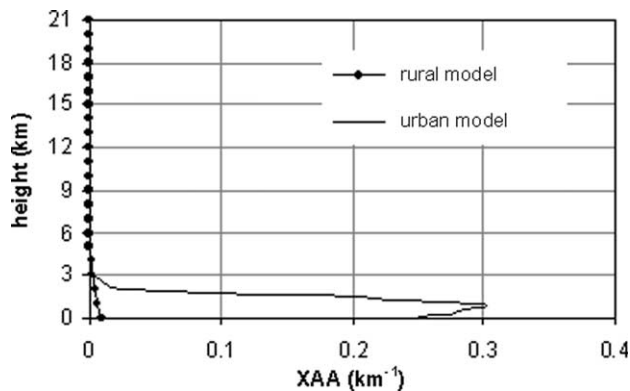


Fig. 5. Aerosol absorption coefficients (XAA) versus the altitude for the rural model and the urban model taken from MODTRAN.

ment. When simulating a zenith-sky measurement one must consider that the distance covered by the photon along the vertical direction before suffering its first scattering, which usually happens within the first few kilometres from the surface, is the shortest it could cover in any other off-axis direction.

Information about the distance covered by photons in every atmospheric layer has been used to compute, according to Eqs. (6) and (7), NO_2 slant columns and air mass factors for the two atmospheric models mentioned above. The curves of SC and AMF displayed in Figs. 6 and 7, respectively, show that the values computed with the rural model are higher than those of the urban model.

The gas vertical profile used in these simulations is the same as that shown in Fig. 1. This is not a secondary aspect to be considered because using a different vertical profile of the absorber would result in different values of both the AMF and SC. Figs. 6 and 7 show that the atmospheric model implemented in the code greatly influences the NO_2 slant column and the air mass factor. This dependence is exaggerated by the trace gas vertical profile used in the simulation. The curves of the AMF and SC shown in Figs. 6 and 7 for the different models would not have been so distinct from each other

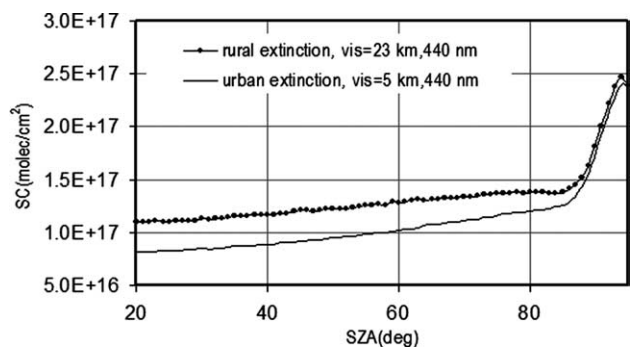


Fig. 6. NO_2 slant columns computed for two different models of atmosphere, as a function of solar zenith angle.

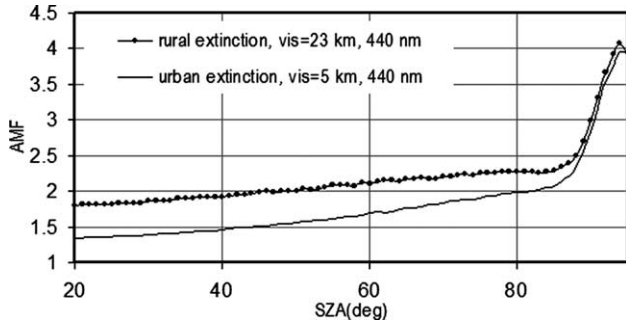


Fig. 7. NO_2 air mass factors computed for two different models of atmosphere, as a function of solar zenith angle.

considering just the climatologic profile of NO_2 which is not characterized by the bulk in the first 2 km.

3.3. A first comparison between the model and the real data

The Gas Analyser Spectrometer Correlating Optical Differences (GASCOD) UV/Vis spectrometer (Evangelisti et al., 1996) installed at ISAC-CNR in Bologna (44.3°N, 11.2°E, 42 m asl), collects zenith scattered solar radiation with a narrow field of view ($<1^\circ$) to measure NO_2 slant column values during sunrise and sunset using DOAS techniques.

In Fig. 8, the NO_2 slant column measured by GASCOD on 19 July 2003 is compared with that simulated

by PROMSAR with the urban aerosol model. The NO_2 vertical profiles used by PROMSAR code for the simulation were obtained by adding to the mid-latitude climatological concentration values a mean concentration of 1, 4 and 8 ppb in the first 500 m from the ground level. These profiles were selected based on the fact that several episodes of high NO_2 concentrations in the lowest troposphere have been observed in campaigns performed in this area in 2003 and that led to the conclusion that the NO_2 mixing layer extends at most up to 500 m (Petritoli et al., 2004).

Fig. 8 clearly shows that the slant column simulated by PROMSAR using the gas profile labelled “ NO_2 4 ppb 0.5 km” (bold solid line) represents very well the curve obtained from real measurements (circles) whereas the slant columns obtained using the other two profiles either underestimated or overestimated the measured slant columns in the whole range of solar zenith angles. Critically analysing graph A, however, it will be noticed that some of the actual measured values fit well to the slant column computed with the gas profile “ NO_2 1 ppb 0.5 km”. This suggests that in the SZA range between 25° and 60° the gas concentration leading to the measured slant column should be between 1 and 4 ppb. This preliminary retrieval is confirmed by the in situ measurements carried out by the Regional Agency for Environmental Protection (ARPA) of Emilia Romagna. The concentration values of NO_2 measured on 19 July 2003 during the afternoon in the suburban stations ranged from 2 to 10 ppb.

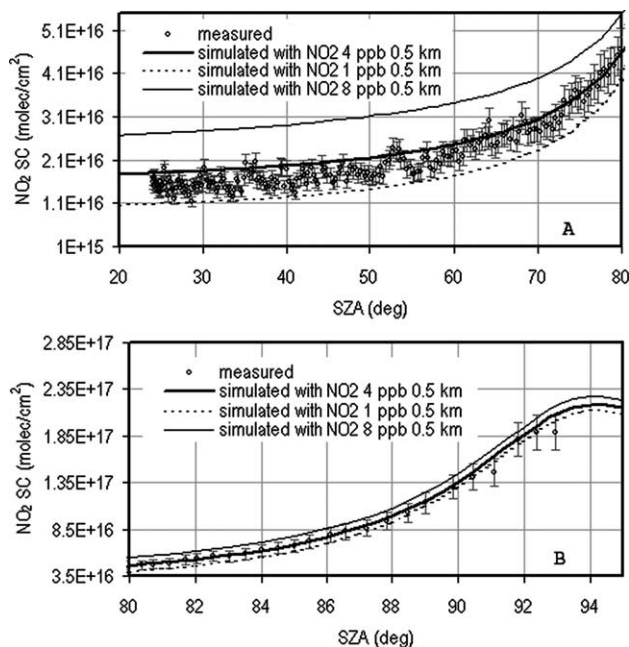


Fig. 8. Comparison between three NO_2 slant columns simulated by PROMSAR and the NO_2 slant column measured at ISAC-CNR (Bologna) on 19/07/2003. The spectrometer GASCOD looking at zenith was located on the roof of the ISAC institute at 42 m of altitude. In A, the interval of solar zenith angles ranges from 20° to 80° , in B from 80° to 95° .

4. Conclusions

PROMSAR is a radiative transfer model for the interpretation of DOAS measurements in the atmosphere. It is based on the Monte Carlo approach which is particularly useful by taking into account multiple scattering processes. In this model, a technique such as the forced collision has been employed for reducing the statistical variance in order to improve computation efficiency.

In this paper, we have presented some applications of the model and a first comparison between a measured NO_2 slant column and that simulated by PROMSAR.

We have verified the sensitivity of PROMSAR in different spectrometer viewing configurations and have concluded that an off-axis line of sight gives longer photon paths in the atmosphere and therefore results in the trace gas air mass factor and slant columns been higher than a zenith sky line of sight.

The possibility of considering a wide variety of atmospheric environments in defining the atmospheric scenario due to the flexibility of MODTRAN is one of the main advantages of PROMSAR. In this paper, we have tested PROMSAR with the rural and urban

atmospheric models and for two different values of visibility. We have proved that the photon paths into every atmospheric layer and the NO₂ slant columns as well as the air mass factors are higher when the rural model is implemented in PROMSAR.

Finally, we have presented the first comparison between a set of slant column values simulated by PROMSAR with different nitrogen dioxide vertical profiles and a real slant column measured at ISAC-CNR on 19 July 2003 with the spectrometer GASCOD installed on the roof of ISAC-CNR institute.

The good agreement between the measured and simulated curves informs us, within the limits of experimental measurements, which was the vertical nitrogen dioxide profile present in the atmosphere at the instant in which measurements were performed.

A very important aspect not to be underestimated in the use of PROMSAR code is the possibility of creating a real database containing the computed mean path of radiation into every atmospheric layer for a given set of solar zenith angles, spectrometer lines of sight, and for a given atmosphere. This database can be used in air mass factor calculation or simulating a slant column and also when the inverse algorithms for the retrieval of the vertical profile of a given trace gas are used.

References

- Berk, A., Anderson, G.P., Acharya, P.K., et al. MODTRAN4 User's Manual. Air Force Research Laboratory, Space Vehicles Directorate, Air Force Materiel Command, Hascom AFB, MA, 1999, pp. 01731–3010.
- Collins, D.G., Blattner, W.G., Wells, M.B., et al. Backward Monte Carlo calculations of the polarization characteristics of the radiation emerging from spherical-shell atmospheres. *Appl. Opt.* 11, 2684–2696, 1972.
- Evangelisti, F., Bonasoni, P., Giovanelli, G., et al. Stratospheric nitrogen dioxide observation at 44°N by UV–VIS DOAS systems, in: Bojkov, R., Visconti, G. (Eds.), *Proceedings of XVIII Quadriennial Ozone Symposium*, vol. 2, pp. 491–491, Parco Sci. e Tecnol. D'Abruzzo, L'Aquila, Italy, 1996.
- Giovanelli, G., Bonasoni, P., Evangelisti, F. Measurements of stratospheric gas absorption in UV and visible spectral regions, in: Colacino, M., Giovanelli, G., Stefanutti, L. (Eds.), *1st Workshop Italian Research on Antarctic Atmosphere. SIF Conference Proceedings*, vol. 20, pp. 197–214, 1989.
- Giovanelli, G., Bonasoni, P., Evangelisti, F. O₃ and NO₂ ground-based measurements at Terra Nova Bay, Antarctica, in: Colacino, M., Giovanelli, G., Stefanutti, L. (Eds.), *2nd Workshop Italian Research on Antarctic Atmosphere. SIF Conference Proceedings*, vol. 27, pp. 255–268, 1990.
- Giovanelli, G., Bonasoni, P., Evangelisti, F. Determination of gas column amount by solar zenith radiation measurements, in: Colacino, M., Giovanelli, G., Stefanutti, L. (Eds.), *4th Workshop Italian Research on Antarctic Atmosphere. SIF Conference Proceedings*, vol. 35, pp. 453–467, 1992.
- Hendrick, F., Van Roozendaal, M., Kylling, A., Wittrock, F., Von Friedeburg, C., Sanghavi, S., Petritoli, A., Denis, L., Schofield, R. Report on the workshop on radiative transfer modeling held at IASB-BIRA, Brussels, Belgium on 3–4 October 2002, report of the QUILT project (EVK2-2000-00545), European Commission, Brussels, 2003.
- Marquard, L., Platt, U. AMFTRAN: A new Monte Carlo radiative transfer model for calculating air mass factors. in: *Proceedings of NATO ARW*, Athens, November 1995. Springer Heidelberg, pp. 231–241, 1997.
- McKenzie, R.L., Johnston, P.V., McElroy, C.T., et al. Altitude distributions of stratospheric constituents from ground-based measurements at twilight. *J. Geophys. Res.* 96, 15499–15511, 1991.
- Noxon, J.F. Nitrogen dioxide in the stratosphere and troposphere measured by ground-based absorption spectroscopy. *Science* 189, 547–549, 1975.
- Palazzi, E. Sviluppo Di Modelli a Supporto Della Metodologia DOAS per La Determinazione Degli Inquinanti in Troposfera. Tesi di laurea, Università di Bologna, 2003 (in Italian).
- Palazzi, E., Premuda, M., Petritoli, A., Giovanelli, G., Kostadinov, I., Ravegnani, F., Bortoli, D. A multiple scattering atmospheric radiative transfer model for diffuse solar radiation measurements along slant polar trajectories, in: Colacino, M. (Ed.), *10th Workshop Italian Research on Antarctic Atmosphere. SIF Conference Proceedings*, vol. 89, pp. 41–58, 2004.
- Petritoli, A. Distribuzioni Verticali Di Gas in Traccia in Atmosfera Ottenute Con Metodi Di Inversione Applicati a Misure Di Quantità Colonnari. Tesi di Laurea, Università di Bologna, 1998 (in Italian).
- Petritoli, A., Giovanelli, G., Kostadinov, I., et al. Tropospheric and stratospheric amount deduced by slant column measurements at Mt. Cimone station. *Adv. Space Res.* 29, 1691–1695, 2002.
- Petritoli, A., Bonasoni, P., Giovanelli, G., et al. First comparison between ground-based and satellite-borne measurements of tropospheric nitrogen dioxide in the Po basin. *J. Geophys. Res.*, 109, 2004, No. D15307.
- Platt, U. Modern methods of the measurements of atmospheric trace gases. *Phys. Chem. Chem. Phys.* 1, 5409–5415, 1999.
- Platt, U., Marquard, L., Wagner, T., et al. Corrections for zenith scattered light DOAS. *Geophys. Res. Lett.* 24, 1759–1762, 1997.
- Preston, K.E., Fish, D.J., Roscoe, H.K., Jones, R.L. Accurate derivation of total and stratospheric vertical columns of NO₂ from ground-based zenith-sky measurements. *J. Atmos. Chem.* 30, 163–172, 1998.
- Roberti, L. Monte Carlo radiative transfer in the microwave and in the visible: biasing techniques. *Appl. Opt.* 36 (30), 7929–7938, 1997.
- Rosanolov, V.V., Kurosu, T., Burrows, J.P. Retrieval of atmospheric constituents in the UV–visible: a new quasi-analytical approach for the calculation of weighting functions. *JQSRT* 60, 277–299, 1998.
- Solomon, S., Schmeltekope, A., Sanders, R.W. On the interpretation of zenith sky absorption measurements. *J. Geophys. Res.* 92, 8311–8319, 1987.
- Stamnes, K., Tsay, S., Wiscombe, W., Jayaweera, K. Numerically stable algorithm for discrete-ordinate-method radiative transfer in multiple scattering and emitting layered media. *Appl. Opt.* 27, 2502–2509, 1988.